

## Pseudo wastewater treatment by combining adsorption and phytoaccumulation on the *Acrostichum aureum* Linn. plant/activated carbon system

Linh Nguyen Thi Truc <sup>a,\*</sup>, Nhu Le Thi Quynh <sup>a</sup>, Vu Duong Ba <sup>a</sup>, Chien Tran Minh <sup>a</sup>, Seungbum Hong <sup>b</sup>, Kwangsoo No <sup>b</sup> and Sunghwan Lee <sup>c,\*</sup>

<sup>a</sup> Department of Chemistry, Ho Chi Minh City University of Education, Vietnam

<sup>b</sup> Department of Materials Science and Engineering, Korea Advanced Institute of Science and Technology, Daejeon, South Korea

<sup>c</sup> School of Engineering Technology, Purdue University, West Lafayette, Indiana, USA

Correspondence: [linhntt@hcmue.edu.vn](mailto:linhntt@hcmue.edu.vn); [sunghlee@purdue.edu](mailto:sunghlee@purdue.edu)

### Abstract

In this study, the pseudo wastewater containing Zn, Fe, Cu ions was clean-up by a combination of physical adsorption onto activated carbon medium and phytoaccumulation using *Acrostichum aureum* Linn. plants. The adsorption capability of the activated carbon for the Fe, Cu, and Zn ions was 3.05, 3.72, and 2.85 mg g<sup>-1</sup>, respectively, at the saturation. The phytoaccumulation performance was proved by analyzing the individual residual ash collected after pyrolysis up to 1000 C of the leaf, stem, and root of the plants. Thermal analyses of thermogravimetry data showed that the weight of the residual ash of the phytoremediated leaf, stem, and root of the plants was 37.0, 19.0, and 65.7 wt.%, respectively. Energy-dispersive X-ray spectroscopy determined the amount of Fe element in the residual ash of phytoremediated root is 7.05 wt.%, while that of the initial root is 1.18 wt.%. Conclusively, it can be proved that combining physical and biological processes is feasible to treat wastewater containing metal ions.

**Keywords:** Phytoaccumulation, activated carbon, wastewater, *Acrostichum aureum* Linn., adsorption.

### 1. Introduction

The excessive release of heavy metals into the environment via general industrial and agricultural activities [2] is one reason for the pollution of water and soil [3]. When the exposed amount of heavy metals is above the permissible limits of humans, they may risk the health conditions. Excess of copper (Cu) ions may disrupt homeostasis and cause disease conditions associated with the hepatic disorder and neurodegenerative alteration. [1]. Free iron can donate or accept an electron from neighboring molecules to damage cellular components that are toxic to the cell [4]. Compared to Cu, Fe ions, zinc is relatively harmless. The accumulation of free zinc at high doses results in a consequence of ischemia or trauma [29]. So far, several technologies, such as precipitation [5], membrane filtration [6–12], ion exchange [13–16], adsorption over other media [17–20], and co-precipitation/adsorption [21], have been employed

1  
2  
3 to clean-up wastewater. Among these methods, the adsorption onto activated carbon (AC) has  
4 been considered as a highly effective technique for the removal of heavy metals from wastewater  
5 [30]. However, the challenge is to achieve a reasonably long service life of AC because of  
6 saturation over time. Therefore, securing a long enough life cycle of AC is a crucial bottleneck  
7 for the potential implementation of the ion adsorption method in purifying wastewater containing  
8 heavy metal species. A system combining AC medium and plants can resolve the current  
9 challenging issue regarding enhancing the service cycle of AC material. This system can be  
10 considered a combination of phytoremediation and adsorption to remove (or reduce) heavy metal  
11 species in wastewater.  
12  
13

14 In Vietnam, as a country located in the tropical zone, mangrove forests are widely prevailing.  
15 The root system of mangrove trees (e.g., *Acrostichum aureum* Linn., *Neem*, *Peepal*, *Maize*,  
16 *Ulmus*, *Araucaria heterophylla*) develops a strong and dominant single main root that grows  
17 vertically into the ground without any critical restriction. The trees grow well on various  
18 substrates, including soil, sediment, or char [23]. In addition, the mangrove trees show the ability  
19 to uptake heavy metal ions through their root system and store the ions in complexes in various  
20 plant compartments [24]. Among these plants, *Acrostichum aureum* Linn. (AAL), which is a fern  
21 of brackish parts of tropical mangrove swamps and grows along the coastal belt in Vietnam [25],  
22 has been considered in phytoremediation in some publications. Dipu Sukumaran *et al.* [26]  
23 evaluated the phytoremediation capability of AAL in the treatment of shrimp farm effluent and  
24 investigated that the parameters including Biochemical Oxygen Demand (BOD), Chemical  
25 Oxygen Demand (COD) and Nitrate ( $\text{NO}_3^-$ ) were significantly reduced during thirty days of the  
26 experimental period. Another publication [27] experimentally proved that AAL can be applied  
27 for the phytoremediation of antibiotic-contaminated sediments. Particularly, a study, by  
28 Kaewtubtim *et al.* [28] on the storage of heavy metals in various parts (leaf, stem, and root) of  
29 AAL plants growing in Pattani Bay, Thailand, reported that the amounts of Cu, Zn, Ni, Mn, Cr,  
30 Pb metals ( $\text{mg}\cdot\text{kg}^{-1}$ ) in AAL stems were measured to be 23.4, 25.1, 21.6, 3.7, 19.1, 6.3  $\text{mg}\cdot\text{kg}^{-1}$ ,  
31 respectively, while their amounts in AAL roots were higher as 41.5, 28.4, 24.3, 23.5, 29.3 and  
32 22.1  $\text{mg}\cdot\text{kg}^{-1}$ . These metals were not detected in AAL leaves. These results confirmed the  
33 accumulation and storage of metal ions in the AAL plants, which demonstrated the potential use  
34 of AAL plants in phytoremediation of heavy metals contaminated wastewater.  
35  
36

37 In this study, we designed a system of AAL plants grown in activated carbon (AC), evaluated the  
38 performance of the AAL/AC system in cleaning up pseudo wastewater containing Fe, Cu, and  
39 Zn ions with a particular concentration. The study aims to demonstrate a potential combination  
40 of physical and biological processes of remediation. The AC plays the role of growing medium  
41 and heavy-metal ion adsorber, and the AAL plants selectively accumulate throughout the  
42 phytoextraction.  
43  
44

## 55 2. Materials and methods

56  
57

### 1 2 3 **Determine the adsorption capacity of the AC**

4  
5 The AC, which is a commercial product made in Vietnam, was prepared in cylindrical granules  
6 with dimensions of diameter, 0.5 cm, and average length, 1.5 cm, as shown in Figure 1a. The  
7 main characteristics of the AC are as follows: the chemical compositions of C 32.3, O 44.7, Al  
8 5.8, Si 13.1 wt.% and other minor elements; the point of zero charges in the range of 8.4 – 8.7;  
9 the surface area of 54.4 m<sup>2</sup>·g<sup>-1</sup>.  
10

11 The pseudo wastewater was formed by dissolving (NH<sub>4</sub>)<sub>2</sub>Fe(SO<sub>4</sub>)<sub>2</sub>·6H<sub>2</sub>O, Zn(CH<sub>3</sub>COO)<sub>2</sub>·2H<sub>2</sub>O,  
12 and CuSO<sub>4</sub>·5H<sub>2</sub>O salts (Aldrich Chemical Co.,) in distilled water. The initial concentration of Fe,  
13 Cu, and Zn ions in the pseudo wastewater was determined to be 465 mg·L<sup>-1</sup>, 420 mg·L<sup>-1</sup>, 309  
14 mg·L<sup>-1</sup>, respectively, measured using Photometer 7100 (Palintest, USA) instrument. The use of a  
15 reagent containing an alkaline thioglycolate reduces ferric iron to ferrous iron, the concentration  
16 of iron in solution is therefore named Fe<sup>2+</sup>.Fe<sup>2+</sup>.  
17

18 40 g AC was introduced to 400 mL pseudo wastewater, continuously stirred, and stably kept at  
19 30 °C. By the hour, 2 mL of solution was taken out, filtered through a  
20 polytetrafluoroethylene (PTFE) syringe filter (0.45 µm pore size). Then, 1 mL of this filtered  
21 solution was diluted with 99 mL distilled water (total 100 mL solution) and measured Fe, Cu,  
22 and Zn concentration via the Photometer 7100 instrument, sequentially.  
23

24 The concentrations of Fe, Cu, and Zn ions adsorbed onto the AC were calculated as follows:  
25

$$26 \quad q_t = \frac{(C_o - C_t) \times V}{D} \text{ (mg·g}^{-1}\text{)} \quad (\text{Eq. 1})$$

27 where,

28 C<sub>o</sub> is the initial concentration of sorbate (mg·L<sup>-1</sup>)  
29

30 C<sub>t</sub> is the remaining concentration of sorbate in solution at any time t (mg·L<sup>-1</sup>)  
31

32 q<sub>t</sub> is the amount of sorbate adsorbed onto the AC at any time t (mg·g<sup>-1</sup>)  
33

34 V is the initial volume of the solution (0.4 L in this study)  
35

36 D is the AC dosage of 40 g.  
37

38 Duplicates were performed for each sample and the relative standard error is equal or less than 3  
39 %.  
40

41 The AC was used as both nutrient-providing growing medium and heavy-metal ion adsorber.  
42 The adsorption capacity of the AC, which is defined as a stored mass (mg) of ions per unit mass  
43 (g) of AC, was determined by monitoring changes in ion mass of the heavy metals.  
44

### 45 **Design the system of AAL plants in the AC (named as the AAL/AC system)**

46 AAL plants, which were collected from Can Gio mangrove forests in Ho Chi Minh City,  
47 Vietnam, have an average length of 50 cm and their leaves with an average size of 2x15 cm<sup>2</sup>.  
48

49 Plastic cylinder vases with dimensions of diameter, 13 cm, and height, 40 cm were used to  
50 contain the AAL/AC system. The solution volume was 2000 mL, and the initial weight of AC  
51 was 1600 g. These vases were connected with small plastic semi-transparent tubes to easily  
52 observe liquid-level inside the vase (Figure 1b). We experimented with ten same vases in the  
53 same condition, and randomly chose three vases to measure independently.  
54



Figure 1: The photographs of (a) the AC and (b) the AAL plants are grown in the AC

#### ***Evaluate the suitability of the AAL/AC system***

The AAL plants grown in the AC were observed every day. Every three days, an appropriate solution (containing  $50 \text{ mg}\cdot\text{L}^{-1}$  for  $\text{NH}_4^+$  and  $50 \text{ mg}\cdot\text{L}^{-1}$  for  $\text{NO}_3^-$ ) was introduced to the system to supply water and nutrients for the plants, which mimics the natural environments and to maintain the liquid level inside the vase. After two months, it was evidenced that the plants grew well, and all leaves were green in healthy conditions with their average length ranging in 25–30 cm, which indicates the plants could steadily grow in the experimental conditions.

The plants were taken out of the vases, and then both the AAL and AC were washed in distilled water to leave out wastes produced during the initial two-month growth. A part of the AAL roots was cut and saved to use as a role of the initial root, which is to be compared with phytoremediated roots grown in pseudo wastewater. Then the AAL plants were grown in the AC again.

#### ***Evaluate the efficiency of the AAL/AC system on phytoremediation in pseudo wastewater***

The pseudo wastewater was introduced into the AAL/AC system. The concentrations of metal ions in the system were continuously monitored using a multi-parameter photometer (Palintest 7100, USA). It must be noted that the  $\text{NH}_4^+$  and  $\text{NO}_3^-$  ions in the wastewater do not affect the measurements of the heavy metal cations of  $\text{Fe}^{2+}$ ,  $\text{Cu}^{2+}$ , and  $\text{Zn}^{2+}$ .

After a month, all the concentrations of ions were completely down to zero. Then, the plants were taken out of the AC to precisely determine the types and amounts of the elements which were stored in various parts of the plants. The plants were divided into three individual parts of the root, branch (stem) and leaf. These parts were dried at  $100^\circ\text{C}$  in a drying oven for one day,

then milled into a powder. TGA/DSC analysis (SETERAM, Labsys Evo, TG–DSC 1600°C) was made on the parts of root, stem, and leaf to investigate the thermal behavior of the compounds containing carbon in the plants. The samples were placed in a platinum cylindrical crucible and heated from 30 to 1000 °C at a ramping rate of 10 K min<sup>-1</sup> using a flow of N<sub>2</sub> (99.99%). The amount of each sample used for the measurements was constant at 28 mg. The compositions of the residual ashes after TGA/DSC were determined using EDX (Horiba H-7593, England).

### 3. Results and discussion

To objectively evaluate the adsorption performance of the AC (by itself, not the AAL/AC system), the metal ion concentrations in the pseudo wastewater were monitored, and the results are shown in Figure 2.

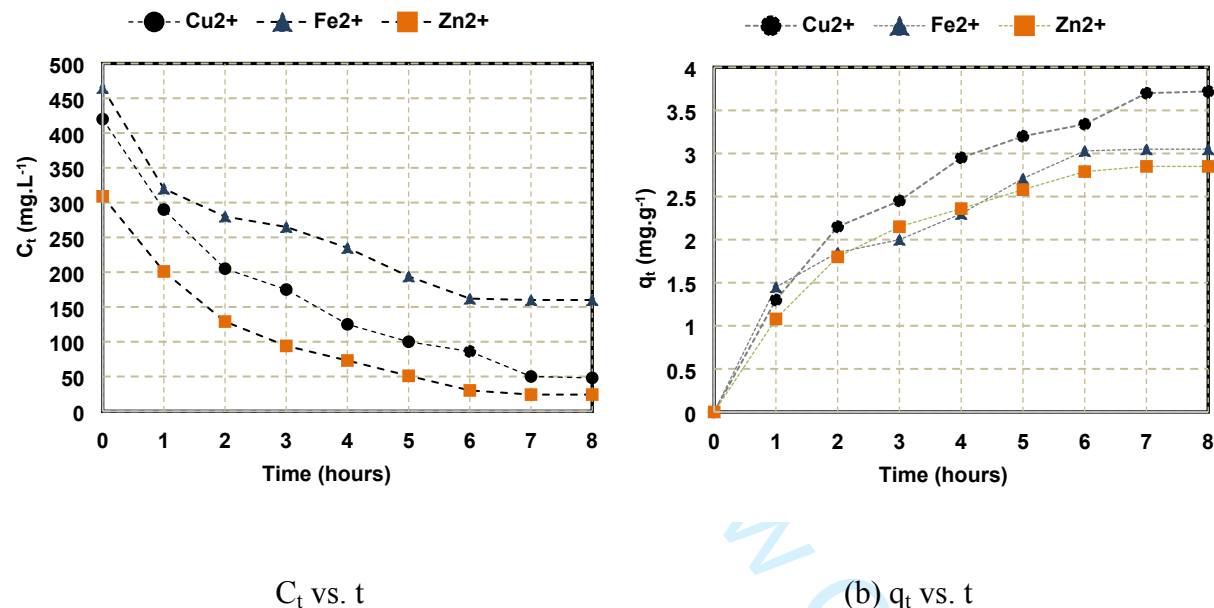


**Figure 2:** (a) A change in concentration ( $C_t$ ) of Fe, Cu, Zn ions in solution as a function of time  
 (b) The amount of the metal ions ( $q_t$ ) adsorbed onto the AC with time

Figure 2a displays a change in concentration of each ion in the solution: the concentrations decrease slowly and lead to a constant value (i.e., saturation) after approximately 7 hours. Overall, 65.6 %, 88.1 %, and 92.2 % of Fe, Cu, and Zn ions, respectively, were adsorbed into the AC with respect to their initial concentration. These results in Figure 2a and Equation (1) were used to determine the adsorption capacity of the AC, which is defined as a stored mass (mg) of ions per unit mass (g) of adsorber (i.e., AC in this study). In Figure 2b, the storing capacities of AC for the Fe, Cu, and Zn ions were determined to be 3.05, 3.72, 2.85 mg·g<sup>-1</sup>, respectively, at the saturation (i.e., at ~ 7 hours). The significance of the results are two-fold: (1) the overall adsorption performance of the AC for Fe, Cu and Zn ions is promisingly high for potential use in phytoremediation, and (2) according to the determined heavy-metal storing capacities (3.05 mg·g<sup>-1</sup> for Fe; 3.72 mg·g<sup>-1</sup> for Cu; 2.85 mg·g<sup>-1</sup> for Zn), the initial AC weight (1600 g),

consequently, has high maximum capabilities to store the heavy–metal Fe, Cu, Zn ions of 4880, 5952, 4560 mg, respectively.

The phytoremediation performance of the AAL/AC system was experimentally evaluated in the pseudo wastewater (containing the initial concentration of Fe, Cu, and Zn ions of  $465 \text{ mg} \cdot \text{L}^{-1}$ ,  $420 \text{ mg} \cdot \text{L}^{-1}$ ,  $309 \text{ mg} \cdot \text{L}^{-1}$ , respectively). To investigate the storage capability of each individual group of the AAL plants (i.e., root, stem and leaf) for the heavy–metal ions and other inorganic elements, TGA/DSC measurements were made on, and the results are shown in Figure 3. In order to exclude the effect of oxidation on the plants due to the presence of  $\text{O}_2$ , the measurements were performed in an inert gas condition with  $\text{N}_2$ .

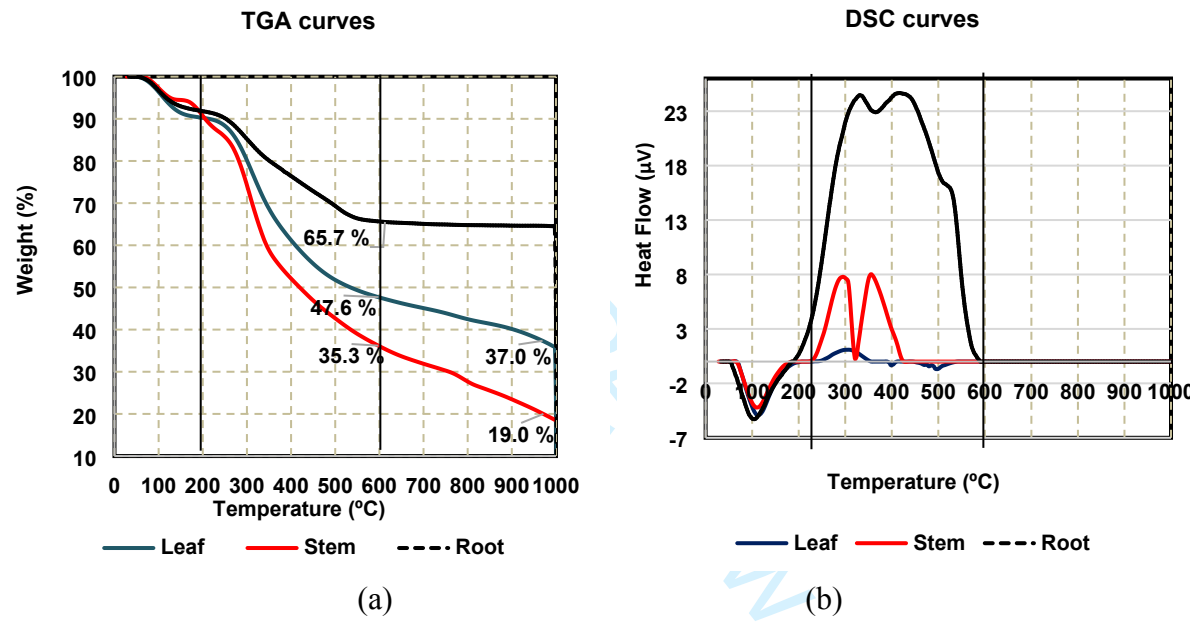


**Figure 3:** (a) TGA curves and (b) DSC curves of the individual parts of the AAL plants after used in phytoremediation

The TGA curves in Figure 3a reveal the weight change (%) with respect to the initial weight, while the DSC curves in Figure 3b indicate the exothermic and endothermic processes during the pyrolysis of the AAL leaf, stem and root parts in  $\text{N}_2$  at temperatures from 25 to 1000 °C. The first weight loss of the three samples starts at around 80 °C and ends at approximately 130 °C (Figure 3a), and, correspondingly, the endothermic peaks are shown in Figure 3b, which are ascribed to the vaporization of water from lignocellulose fibers [31]. At 200 °C, the weight loss of the AAL leaf, stem, and the root is similar – around 10 wt.% loss for all the groups. However, the thermal behaviors of the three groups become significantly different at a temperature from 200 °C to 600 °C. The total weight loss (initial 100% – residual ash wt.% remaining at 600 °C) of the AAL leaf, stem, and root at 600 °C was found to be 52.4, 64.7, and 34.3 wt.%, respectively (Figure 3a). Correspondingly, Figure 3b shows the DSC curve of the root sample with a large overlap of

exothermic peaks which is attributed to full pyrolysis of compounds containing carbon (such as cellulose, hemicellulose, lignin or other compounds [32,33]), while the DSC curves of the leaf and stem specimens display smaller exothermic peaks due to incomplete organic pyrolysis. At temperatures higher than 600 °C, no significant weight loss is observed in the root TGA curve, which is consistent with the DCS results in Figure 3b, where no endothermic or exothermic peaks are seen. The TGA curves of the leaf and stem samples, however, show a monotonic decrease in weight at temperatures higher than 600 °C. As a result, the weight of the residual ash of AAL leaf, stem, and root at 1000 °C was measured to be 37.0, 19.0, and 65.7 wt.%, respectively. These significant differences in weight after pyrolysis between the parts of AAL plants is likely attributed to the different amounts of inorganic compounds (in either form of oxides or salts) in each part that is thermally stable up to 1000 °C during pyrolysis. Therefore, we hypothesize that the different weights of the parts after pyrolysis pertain to the absorption characteristics of the AAL plant – i.e., according to the high weight % remaining in the root, the AAL root may absorb different species from those absorbed by the AAL leaf and stem.

To precisely determine the types of elements in the residual ash after pyrolysis, EDX measurements were made in the three groups of phytoremediated samples and apart from the initial root. To compare the elemental compositions of the phytoremediated root, the initial root (non-phytoremediated) was also investigated with EDX. The results are shown in Table 1 and Figure 4.

**Table 1:** The components (wt.%) of the residual ashes

| Element     | Leaf  | Stem  | Root<br>(phytoremediation) | Root<br>(initial) |
|-------------|-------|-------|----------------------------|-------------------|
| <b>C K</b>  | 44.36 | 35.73 | –                          | 27.18             |
| <b>O K</b>  | 31.14 | 31.42 | 50.95                      | 40.93             |
| <b>Na K</b> | 5.31  | 7.40  | –                          | 1.04              |
| <b>Mg K</b> | 1.59  | 1.11  | 0.94                       | –                 |
| <b>Al K</b> | –     | 0.71  | 10.67                      | 7.92              |
| <b>Si K</b> | 9.58  | 8.72  | 28.62                      | 20.40             |
| <b>P K</b>  | 0.32  | –     | –                          | –                 |
| <b>S K</b>  | 0.61  | 0.34  | –                          | –                 |
| <b>Cl K</b> | 2.53  | 3.98  | –                          | –                 |
| <b>K K</b>  | 2.47  | 7.15  | 1.77                       | 1.25              |
| <b>Ca K</b> | 2.08  | 3.44  | –                          | –                 |
| <b>FeK</b>  | –     | –     | 7.05                       | 1.18              |

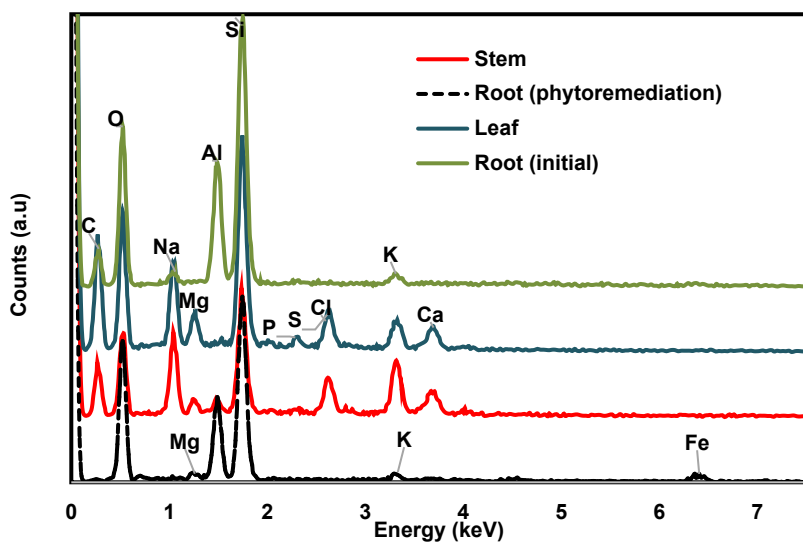
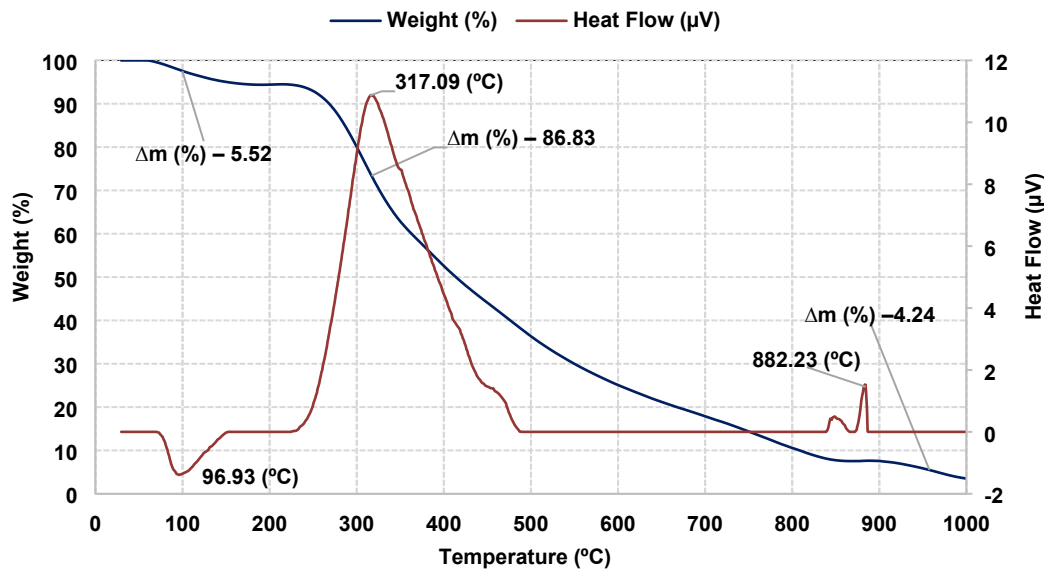


Figure 4: EDX spectra of the residual ashes of leaf, stem and roots (initial and phytoremediated)

In Table 1, the residual ashes from the leaf and stem contain very similar elements including Na, Mg, Si, S, Cl, K, Ca at similar concentrations (except the minor concentration of P for leaf and Al for stem) while the phytoremediated root is found to be significantly different from those of the leaf and stem. The concentrations of Al, Fe, and Si elements in the phytoremediated root are considerably higher than those in the leaf and stem residual ashes. Since the initial root naturally contains Al and Si elements at high concentrations, 7.92 wt.% for Al and 20.40 wt.% for Si, the elemental analysis for phytoremediated root serves as evidence that the roots of AAL plants selectively take up Fe ions. No carbon is detected in the phytoremediated root, unlike the high amounts of carbon, 44.36 wt.% for leaf and 35.73 wt.% for the stem. This result is due to the full pyrolysis of organic compounds containing carbon in the phytoremediated root, which is in good agreement with the TGA/DSC results in Figure 3. Frequently, the role of Al and Si for pyrolysis exhibits when these elements belong to the crystalline structure of zeolite (e.g., ZSM-5) or silicate alumina materials as catalytic carriers. However, in the current study, Al and Si elements are in separated oxides, not in crystals of zeolite. Therefore, it is hypothesized that the demonstrated full pyrolysis is likely facilitated by the catalytic effect of Fe in the phytoremediated root. The hypothesis is supported by several previous reports in the literature where similar results of significantly reduced carbon compounds are shown due to the impregnation of Fe [34-36]. Further studies of the Fe catalytic performance for pyrolysis are underway.

In order to objectively assess the phytoremediation ability of the system suggested in this study, it is required to determine the origin of Fe in the root: either naturally available or formed during phytoremediating process. To answer the question, the thermal behavior of the initial root (non-phytoremediated) was investigated, and the resulting TGA/DSC curves are presented in

Figure 5 to compare the thermal behaviors with those of phytoremediated root shown in Figure 3. The component comparison of the two residual ash samples (phytoremediated vs. initial) is also available from the EDX results in Figure 4 and Table 1: the amount of Fe element in the residual ash of phytoremediated root is 7.05 wt.%, while that of the initial root is 1.18 wt.%.



**Figure 5:** TGA/DSC curves of the initial root

The initial root's DSC curve in Figure 5 also has an endothermic peak at 96.93 °C ascribed to the vaporization of water (as shown in the phytoremediated root), exothermic peaks ranging in 230 to 500 °C, 840 to 865 °C and 870 to 890 °C attributed to the charring process of organic compounds. The TGA curve shows three steps of weight loss (with the values at the first, second, and third steps are 5.5, 86.8, and 4.2 wt.%, respectively), and the total amount of residual ash is below 5 wt.%. In Figure 3a, the weight of residual ash from the phytoremediated root is kept constantly at temperatures higher than 600 °C (65.7 wt.%, without carbon). However, in the left axis of Figure 5, the weight of the initial root at 600 °C is approximately 25 wt.% and continuously decreases to 5 wt.% (of which the carbon concentration is 27.18 wt% (Table 1)) at 1000 °C. Therefore, similar to **the leaf and stem's thermal behavior**, the TGA and EDX results investigate the incomplete organic pyrolysis of the initial root. On the other hand, Table 1 shows the amount of Fe in the phytoremediated root is six times higher than that in the initial root, while Cu and Zn are not **detected**. It is deduced that the amount of Fe in the root is formed via **the phytoremediation process**, while the accumulation of Cu, Zn ions cannot be determined.

#### 4. Conclusion

To demonstrate a potential combination of physical and biological processes of remediation, we designed the AAL plant/AC system, independently determined the AC's adsorption capacity, and proved the AAL plants' phytoremediation in the system. The results showed that the AC could play the role of growing medium and of a metal ion adsorbent thanks to its appropriate

1  
2  
3 adsorption capacity ( $3.05 \text{ mg}\cdot\text{g}^{-1}$  for Fe,  $3.72 \text{ mg}\cdot\text{g}^{-1}$  for Cu, and  $2.85 \text{ mg}\cdot\text{g}^{-1}$  for Zn). The  
4 AAL plants grow well in the AC medium, selectively accumulate Fe ions in the roots, which was  
5 detected via EDX and TGA/DSC techniques. However, these techniques cannot detect Cu and  
6 Zn ions in the leaf, stem, and roots. We claim that almost metal ions were adsorbed and stored in  
7 the AC medium. The inexpensive and eco-friendly AAL/AC system is appropriate to many  
8 developing and underdeveloped countries that suffer from water contaminated by metal ions  
9 such as Cu, Zn, Fe.  
10  
11

### Acknowledgement

12  
13 This work is supported by Basic Science Research Programs (No. 2015R1D1A1A01056983)  
14 through the NRF, Korea, funded by the Ministry of Education, and (CS. 2020. 19. 19) funded by  
15 Ho Chi Minh City University of Education, Vietnam.  
16  
17

### References

18  
19  
20  
21 [1] Gaetke LM, Chow-Johnson HS, Chow CK. Copper: toxicological relevance and  
22 mechanisms. *Archives of toxicology*. 2014;88(11):1929–1938.  
23  
24 [2] Kadirvelu K, Thamaraiselvi K, Namasivayam C. Removal of heavy metal from industrial  
25 wastewaters by adsorption onto activated carbon prepared from an agricultural solid waste.  
26 *Bioresource Technology*. 2001;76:63–65.  
27  
28 [3] Baker AJM, Reeves RD, Hajar ASM. Heavy metal accumulation and tolerance in British  
29 populations of the metallophyte *Thlaspi caerulescens* J. & C. Presl (Brassicaceae). *The New*  
30 *Phytologist*. 1994;127:61–68.  
31  
32 [4] Rawan E, Nagla TT, Michael TG. Iron mediated toxicity and programmed cell death: A  
33 review and a re-examination of existing paradigms. *Biochimica et Biophysica Acta (BBA) -*  
34 *Molecular Cell Research*. 2017;1864(2):399-430.  
35  
36 [5] Madeline S, Andrea H. Life cycle assessment review of struvite precipitation in wastewater  
37 treatment. *Resources. Conservation and Recycling*, 2018;139:194–204.  
38  
39 [6] Rizwan A, Muhammad A, Eunyoung P, et al. Submerged low-cost pyrophyllite ceramic  
40 membrane filtration combined with GAC as fluidized particles for industrial wastewater  
41 treatment. *Chemosphere*. 2018;206:784–792.  
42  
43 [7] Sarah K, Adnan Q, Johannes SV, et al. Fouling resilient perforated feed spacers for  
44 membrane filtration. *Water Research*. 2018;140:211–219.  
45  
46 [8] Zhuoyan H, Dehua X, Yajing H, et al. 3D MnO<sub>2</sub> hollow microspheres ozone-catalysis  
47 coupled with flat-plate membrane filtration for continuous removal of organic pollutants:  
48 Efficient heterogeneous catalytic system and membrane fouling control. *Journal of Hazardous*  
49 *Materials*. 2018;344:1198–1208.  
50  
51 [9] Laura B, Vincenzo N, Marwa SS, et al. Wastewater treatment by membrane ultrafiltration  
52 enhanced with ultrasound: Effect of membrane flux and ultrasonic frequency. *Ultrasonics*.  
53 2018;83:42–47.  
54  
55  
56  
57  
58  
59  
60

[10] Mashallah R, Afsaneh K, Mohammad M. Membrane filtration of wastewater from gas and oil production. *Environmental Chemistry Letters*. 2018;16

[11] Onur I, Amr MA, Hale O, et al. Comparative evaluation of ultrafiltration and dynamic membranes in an aerobic membrane bioreactor for municipal wastewater treatment. *Environmental Science and Pollution Research*. 2019;1–11.

[12] Weilong S., Zhipeng L., Yi D., et al. Performance of a novel hybrid membrane bioreactor for treating saline wastewater from mariculture: Assessment of pollutants removal and membrane filtration performance. *Chemical Engineering Journal*. 2018;331:695–703.

[13] Ahsan M, Ana S, Bruce J. The impact of background wastewater constituents on the selectivity and capacity of a hybrid ion exchange resin for phosphorus removal from wastewater. *Chemosphere*. 2019;224:494–501.

[14] Farshad M., Rajesh GP, Behnam K, et al. Efficient treatment of oil sands produced water: Process integration using ion exchange regeneration wastewater as a chemical coagulant. *Separation and Purification Technology*. 2019;221:166–174.

[15] Anthony M, Ahmad A, Stephen JA. Ion exchange homogeneous surface diffusion modelling by binary site resin for the removal of nickel ions from wastewater in fixed beds. *Chemical Engineering Journal*. 2019;358:1–10.

[16] Ian BR, Sabolc P, Dagmar S, et al. Comparison of sustainable biosorbents and ion–exchange resins to remove  $\text{Sr}^{2+}$  from simulant nuclear wastewater: Batch, dynamic and mechanism studies. *Science of The Total Environment*. 2019;650(2):2411–2422.

[17] Hua T, Haynes RJ, Zhou YF. Potential use of two filter media in constructed wetlands for simultaneous removal of As, V and Mo from alkaline wastewater – Batch adsorption and column studies. *Journal of Environmental Management*. 2018;218:190–199.

[18] Liu J, Zhu X, Zhang H, et al. Superhydrophobic coating on quartz sand filter media for oily wastewater filtration. *Colloids and Surfaces A: Physicochemical and Engineering Aspects*. 2018;553:509–514.

[19] Alexander EB, Evgeny VG, Irina VB, et al. Adsorption of heavy metals on conventional and nanostructured materials for wastewater treatment purposes: A review. *Ecotoxicology and Environmental Safety*. 2018;148:702–712.

[20] Babel S, Kurniawan TA. Low–cost adsorbents for heavy metals uptake from contaminated water: a review. *Journal of Hazardous Materials*. 2003;97:219–243.

[21] Hala AH. Removal of heavy metals from wastewater using agricultural and industrial wastes as adsorbents. *HBRC Journal*. 2013;9(3):276–282.

[22] Prasad MNV, Freitas H. Metal hyperaccumulation in plants–Biodiversity prospecting for phytoremediation technology. *Electronic Journal of Biotechnology*. 2003;6(3):285–321.

[23] Hossain MD, Nuruddin AA, Soil and Mangrove: A Review. *Journal of Environmental Science and Technology*. 2016;9:198–207.

[24] Kaewtubtim P, Meeinkuirt W, Seepom S, et al. Heavy metal phytoremediation potential of plant species in a mangrove ecosystem in Pattani bay, Thailand. *Applied Ecology and Environmental Research*. 2016;14(1):367–382.

[25] Baba S, Chan HT, Aksornkoae S. Useful Products from Mangrove and other Coastal Plants. ISME Mangrove Educational Book Series No. 3. International Society for Mangrove Ecosystems (ISME), Okinawa, Japan, and International Tropical Timber Organization (ITTO), Yokohama, Japan. 2013

[26] Dipu S, Justy J, Madhavan K, et al. The Role of Antioxidant Metabolism in Phytoremediation of Shrimp Farm Effluent by *Acrostichum aureum* Linn. *American Journal of Environmental Protection*. 2019;7(1):7–12.

[27] Thuy TTH, Loan TCT, Nga PL, et al. A Preliminary Study on The Phytoremediation of Antibiotic Contaminated Sediment. *International Journal of Phytoremediation*. 2013;15(1):65–76.

[28] Kaewtubtim PW, Meeinkuirt W, Meeinkuirt SSJ, et al. Heavy metal phytoremediation potential of plant species in a mangrove ecosystem in Pattani Bay, Thailand. *Applied Ecology and Environmental Research*. 2016;14(1):367–382.

[29] Frederickson CJ, Koh JY, Bush AI. The neurobiology of zinc in health and disease. *Nat Rev Neurosci*. 2005;6(6):449-462.

[30] Chand S, Aggarwal VK, Kumar P. Removal of hexavalent chromium from the wastewater by adsorption. *Indian Journal Environment Health*. 1994;36(3):151-158.

[31] Daniel L, Matthias H, Hartmut O, et al. Quantitative and Qualitative Analysis of Surface Modified Cellulose Utilizing TGA-MS. *Materials (Basel)*. 2016;9(6):415.

[32] Ball R, McIntosh AC, Brindley J. Feedback processes in cellulose thermal decomposition: implications for fire-retarding strategies and treatments. *Combust Theor Model*. 2004;8:281–291.

[33] Moran JI, Alvarez VA, Cyrus VP, et al. Extraction of cellulose and preparation of nanocellulose from sisal fibers. *Cellulose*. 2008;15:149–159.

[34] François XC, Ammar B, Martin D, et al. Influence of impregnated iron and nickel on the pyrolysis of cellulose. *Biomass and Bioenergy*. 2015;80:52-62.

[35] Bru K, Blin J, Julbe A, et al. Pyrolysis of metal impregnated biomass: An innovative catalytic way to produce gas fuel. *Journal of Analytical and Applied Pyrolysis*. 2007;78(2):291-300.

[36] François XC, Joël B, Ammar B, et al. Influence of impregnated metal on the pyrolysis conversion of biomass constituents. *Journal of Analytical and Applied Pyrolysis*. 2012;95:213-226.